Penerbit Akademia Baru

Journal of Advanced Research in Fluid Mechanics and Thermal Sciences

Journal homepage: www.akademiabaru.com/arfmts.html
ISSN: 2289-7879

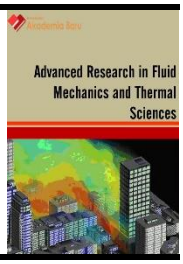

Investigation of Newtonian and Power-Law Blood Flow Models in a 180° Curved Pipe at Low to Medium Shear Rate

Open Access

Samar Ahmed Mahrous[1,2,*], Nor Azwadi Che Sidik[3], Khalid Mansour Saqr[2,4]

[1] Department of Thermo-fluid Universiti Teknologi Malaysia, 81310 UTM Skudai, Malaysia
[2] College of Engineering and Technology, Arab Academy for Science, Technology and Maritime Transport, P.O.BOX 1029 Alexandria, Egypt
[3] Malaysia – Japan International Institute of Technology (MJIIT), University Teknologi Malaysia Kuala Lumpur, 54100 Kuala Lumpur, Malaysia
[4] Research Center for Computational Neurovascular Biomechanics (RCCNB), Alexandria University Hospital in Smouha, 21554 Alexandria, Egypt

ARTICLE INFO

Article history:
Received 23 December 2019
Received in revised form 2 February 2020
Accepted 4 February 2020
Available online 9 April 2020

ABSTRACT

The purpose of this brief paper is to obtain quantitative information on mean velocity profile in ideal vasculature (i.e. straight and toroidal pipes) at low to medium shear rates. To shed the light on the significance of considering blood shear-thinning properties, the power-law model is compared to the commonly used Newtonian viscosity hypothesis. Validated CFD models of blood flow were established and parameterized to solve steady incompressible blood flow under Reynolds number of 50~200. The calculations of the Reynolds number and boundary conditions adopted the shear-thinning index of the power-law models to provide physically correct benchmark for the comparison presented herein. Velocity profiles for Newtonian and non-Newtonian fluid flow are described and sketched. Shear rate values had a range of 20~200 s^{-1} which represents the physiological range found in cerebral vasculature. This study provides the means to estimate the effect of the non-Newtonian properties of the blood on the flow patterns. It is clearly shown that the difference between Newtonian and power-law blood flow models is not significantly affected by Reynolds number for the current range of shear rate. The differences identified in the pressure-drop per unit length and average wall-shear stress were found to be of significant values. The difference between the Newtonian and power-law model (case1) in the pressure drop per unit length for the straight pipe was 386 while for the curved pipe was 371. These differences increased to 538 at Re=200 for the straight pipe and reached 603 for the curved pipe. This research suggests that the non-Newtonian effects of cerebral blood flow should be considered in the respective CFD models.

Keywords:
non-Newtonian fluid; CFD; shear rate; average wall shear stress; pressure drop

1. Introduction

Blood shows non-Newtonian behaviour as a result of its complex mixture of proteins and of suspended cellular elements in plasma [1,2]. However, several studies have considered blood as a

* *Corresponding author.*
E-mail address: samar.mahrous@aast.edu (Samar Ahmed Mahrous)

https://doi.org/10.37934/arfmts.69.1.148162

Newtonian fluid under the justification that in large arteries the rheological properties of blood become linear when shear rate is greater than 100 s^{-1} [3-7]. The non-Newtonian flow effects could become significant when the shear rate is below 100 s^{-1} [8].

Non-Newtonian flows are very important in many disciplines [9-14]. Blood exhibit non-Newtonian characteristics including shear-thinning and viscoelasticity, but in this study, we will focus on the shear-thinning behaviour. Several studies have presented that viscoelastic behaviour is only noticeable in pulsatile flow [15], and that viscoelasticity is only substantial at shear rates less than $10s^{-1}$ [16]. Studies revealed that WSS is an important hemodynamic factor in intracranial aneurysm genesis, growth and rupture [17-20]. The most important parameter that affect the WSS is the blood viscosity. Previous works proved that there is an overestimation of the WSS, when neglecting the effect of the shear-thinning in the simulation [21,22]. On the contrary, some discovered that there is an underestimation of the WSS by neglecting the shear-thinning [23,24]. The effect of four non-Newtonian models (Casson, generalized power law, and the two form of Carreau models) have been investigated by studying the WSS of cerebral aneurysms [25]. It is found that all the non-Newtonian models report a lower WSS than that obtained with a Newtonian model in the same geometry. Additionally, they found that the Carreau model is the most conservative predictor of aneurysm vulnerability as well. Johnston *et al.,* [26] studied five non-Newtonian blood models (power-law, Carreau, walburn-schneck, casson and generalized power law), as well as the usual Newtonian model of blood viscosity to determine the wall shear stress in four different right coronary arteries at a particular point in the cardiac cycle. It was found that the Newtonian model of blood viscosity is a good approximation in regions of midrange to high shear greater than 100 s^{-1}, it is recommended to use the Generalised Power Law model (which tends to the Newtonian model in those shear ranges in any case) in order to reach better approximation of wall shear stress at low shear less than 100 s^{-1}. Some authors concluded that the non-Newtonian behavior for flow in large arteries is crucial [27-29] while others found it is insignificant assumption [30,31]. Gijsen *et al.,* [29] highlighted several differences in the velocity profiles between Newtonian and non-Newtonian models when they investigated the blood flow through 90° curved tube. It is more accurate to include the shear-thinning non-Newtonian property of blood viscosity [32,33]. Xiao Liu *et al.,* investigated the effect of the non-Newtonian (Carreau model) pulsatile blood flow on the transports of oxygen and low density lipoproteins (LDLs) in the human aorta and compared the results with those of the Newtonian steady blood flow [34]. Results showed that the shear thinning nature of blood has small effect on LDL and oxygen transport in most regions of the aorta, but in the atherogenic-prone areas where luminal surface LDL concentration is high and oxygen flux is low, its effect is significant. In addition, Durairaj *et al.,* [35] reported that the non-Newtonian behavior of blood has a significant influence on the WSS value in human aorta. Thus, the non-Newtonian properties should be considered, when simulating the blood flow in aorta. The effect of the blood viscosity changes due to hematocrit (Hct) variations and for a wide range of shear rate on the oxygen transport in a stenosed artery after angioplasty has been studied [36]. Results revealed that the oxygen transport in this constricted artery is significantly influenced by the non-Newtonian shear-thinning (Carreau model) property of blood viscosity with different Hct concentrations. This study has significant implications for drug therapy related to blood-thinning medication. A numerical study has shown that the blood's nonlinear non-Newtonian (Carreau-Yasuda) properties resulted in more accurate predictions of wall shear stress than the Newtonian model within a stented artery [37]. Therefore, the blood's nonlinearity plays an important role, and that the Newtonian model is not appropriate to be used to model the blood flow. The purpose of this paper is to elucidate the difference between Newtonian and power-law blood flow models at shear rate values corresponding to such found in cerebral vasculature. The importance of

this work is driven by the ongoing debate in literature regarding the viability of modelling the non-Newtonian effects in cerebral vessels.

2. Mathematical Model and Numerical Approach

2.1 Governing Equation

The flow field is assumed to be incompressible, steady and three dimensional. The governing equations are the continuity equation (conservation of mass) and the momentum equation in the three dimensions (conservation of momentum).

$$\nabla . v = 0 \tag{1}$$

$$\rho(v . \nabla v) = -\nabla p + \nabla . \tau \tag{2}$$

where, v is the velocity vector field of the fluid, p is the pressure, ρ is the density of the blood 1060 kg/m^3 and τ is the stress tensor. The stress tensor is related to the strain rate tensor ($\dot{\gamma}$) as follows,

$$\tau = \mu \dot{\gamma} \tag{3}$$

where

$$\dot{\gamma} = (\frac{\partial v_i}{\partial x_j} + \frac{\partial v_j}{\partial x_i}) \tag{4}$$

For the Newtonian flow model, the value of blood viscosity is constant $\mu = 0.0035$ Pa.s [38-41]. More refined models, e.g., the power-law model, the Carreau model, the cross model and the Carreau-Yasuda model, include the shear-thinning behavior of blood which capture the non-Newtonian rheology. In this study the proposed Power-law model, is used to account for the shear-thinning behavior of the blood [42-44].

$$\mu = k \dot{\gamma}^{n-1} \tag{5}$$

where, μ is the dynamic viscosity, k is the flow consistency index, $\dot{\gamma}$ is the shear rate and n is the power law index. The model parameters are listed in Table 1.

Table 1
Power-Law model Parameters

Cases	k ($Pa.s$^n)	n
Case 1	0.035	0.6
Case 2	0.01467	0.7755

The Reynolds number is calculated based on (6) and (7) for the Newtonian and non-Newtonian viscosity models respectively. Table 2 provides a summary for the corresponding mean velocity at different Reynolds number for the Newtonian and non-Newtonian viscosity models. Many previous studies might not have used the correct way to calculate the Reynolds number for non-Newtonian fluid such as [45,46].

$$Re = \frac{\rho u_m d}{\mu} \tag{6}$$

$$Re_{NN} = \frac{\rho {u_m}^{2-n} d^n}{k}$$ [42,47] (7)

Table 2
The corresponding mean velocity at different Reynolds number for the Newtonian and non-Newtonian viscosity models

Reynolds number Re	u_m (m/s) Newtonian model	u_m (m/s) non-Newtonian model (case 1)	u_m (m/s) non-Newtonian model (case 2)
50	0.033	0.0997	0.0753
100	0.066	0.164	0.133
200	0.132	0.268	0.233

2.2 Models Geometry

The first stage concerning modelling flow in more realistic vessel shapes is to study simple geometries such as straight pipe (case 1) and curved pipe (case 2) in order to mimic the intracranial arteries. Both structured models were meshed using GAMBIT software (meshing generator). Table 3 provides a summary for the geometries.

2.2.1 Straight pipe

The geometry used in validation cases for Newtonian and Non-Newtonian models of flow of blood is a simple rigid straight pipe as that shown in Figure 1 with length of 0.1m and a diameter of 0.005m.

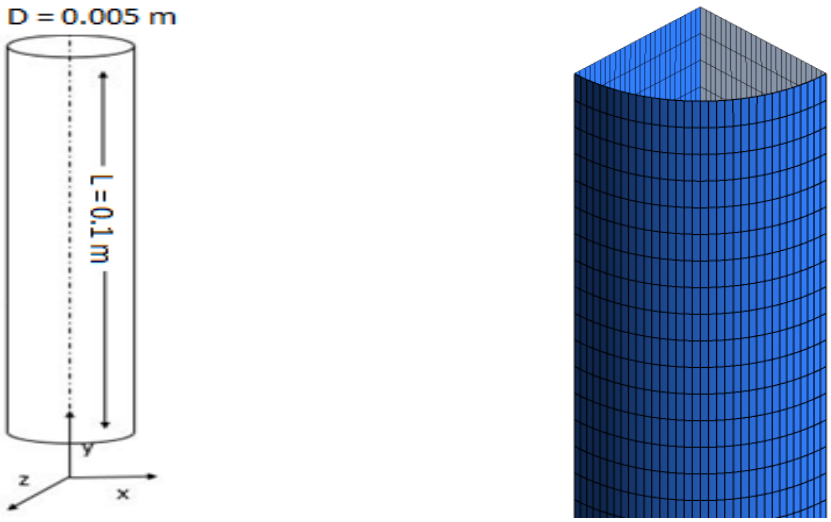

(a) (b)

Fig. 1. (a) Ideal geometry used in straight pipe, (b) meshing

2.2.2 Curved pipe

The curved pipe used to model the flow of is shown in Figure 2 with a diameter of 0.005m. Several models with different grid sizes were tested and the result of the grid independence study was a grid with a total number of elements 300000 elements with 10 boundary layers have been attached to the walls of the curved pipe thus ensuring accurate computation, with interval size equal to 0.06 (mm). The wall of the pipe is assumed to be rigid. The velocity profiles of all models were plotted on

five locations, as shown in Figure 2. The velocity profiles are compared at different Reynolds number in Figures 6-10. The pulsatility of the flow was not included in this study.

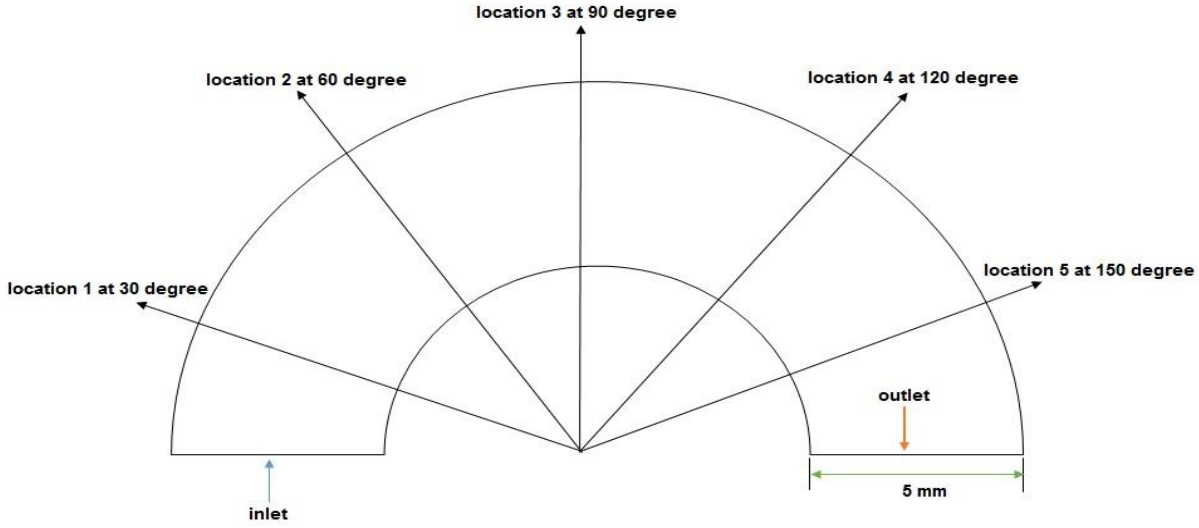

(a)

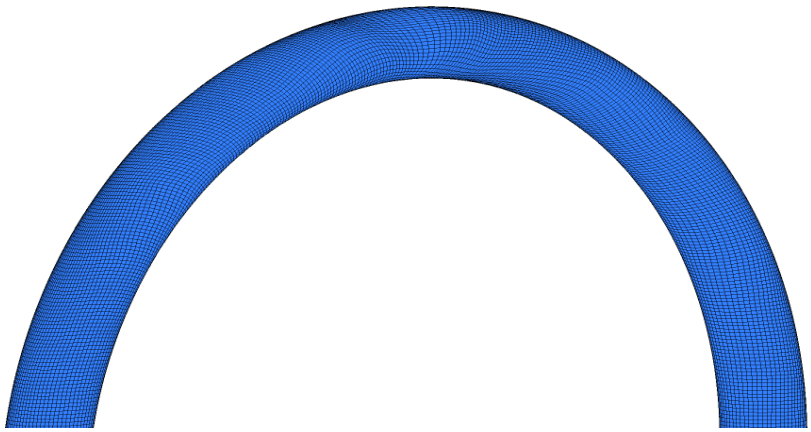

(b)

Fig. 2. (a) Ideal geometry used in curved pipe, (b) Meshing

Table 3
Summaries of geometries

Grid	Number of elements	Element shape	Turning angle	Dimension
Straight pipe	150000	Hexahedral	0	D=5mm
Curved pipe	300000	Hexahedral	180^0	D=5mm

2.3 Mesh Sensitivity Analysis

An analysis of mesh sensitivity was firstly carried out with a steady flow condition. The mesh refinement was confirmed with several mesh systems with the element number increasing up to 200000 cells for the straight pipe and up to 0.5 million for the curved pipe based on the velocity profile. The velocity difference in-between 50000 ~ 200000 elements for the straight pipe and 100000 ~ 0.5 million elements for the curved pipe were less than 2%. This is made to make sure that the cells larger number do not affect the simulation results. For the straight pipe, the results are similar when used 200000 cells and 150000 cells as shown in Figure 3. However, it was slightly different when used 100000 cells, so the 150000 hexahedral cells considered for simulation.

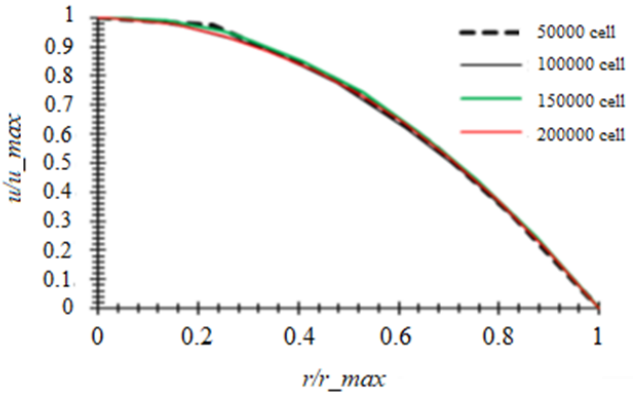

Fig. 3. Mesh Sensitivity Test (Re=200) of straight pipe

2.4 Boundary Condition

The model has one inlet (velocity inlet) and one outlet (pressure outlet, P = 0 pa) with no slip boundary condition and the wall of the pipe was assumed to be rigid.

2.4.1 The Newtonian case

For the Newtonian case, the inlet velocity profile is the fully developed Hagen-Poiseuille flow.

$$u(r) = u_m(1 - \frac{r^2}{R^2}) \tag{8}$$

2.4.2 The non- Newtonian case

For the non-Newtonian case, the inlet velocity profile is the fully developed Power-law pipe flow [42,47-51].

$$u(r) = \frac{n}{n+1}(\frac{dp}{dz}\frac{1}{2k})^{\frac{1}{n}}[R^{\frac{n+1}{n}} - r^{\frac{n+1}{n}}] \tag{9}$$

$$u_m = \frac{n}{n+1}(\frac{dp}{dz}\frac{1}{2k})^{\frac{1}{n}}R^{\frac{n+1}{n}} \tag{10}$$

$$\frac{u(r)}{u_m} = 1 - (\frac{r}{R})^{\frac{n+1}{n}} \tag{11}$$

$$u(r) = u_m\left[1 - (\frac{r}{R})^{(\frac{n+1}{n})}\right] \tag{12}$$

2.5 CFD FLUENT Solver Implementation and Numerical Schemes

The models used in this study were 3D model, incompressible, laminar and steady. The governing equations described before were discretized by the finite volume method. The numerical simulation was carried out with the ANSYS package (FLUENT 16). No turbulence model was applied due to the relatively low Reynolds number in this study. Each model required approximately 4 days of CPU time

on an HPC with a 4 Intel Xeon (2.6GHz); parallel computation with a cluster on 32 nodes was carried out with Platform Computing. The convergence criteria for iterative errors were set to be of 1×10^{-6}.

2.6 Validation with Exact Solution

The model has been validated for the steady Newtonian and non-Newtonian (Power-law) against the exact solution of the fully developed pipe flow (Hagen-Poiseuille solution) Figure 4 and Figure 5 respectively, at Reynolds number (Re) =100. The numerical results agree well with the exact solution with error less than 2%.

2.6.1 Validation of the Newtonian case

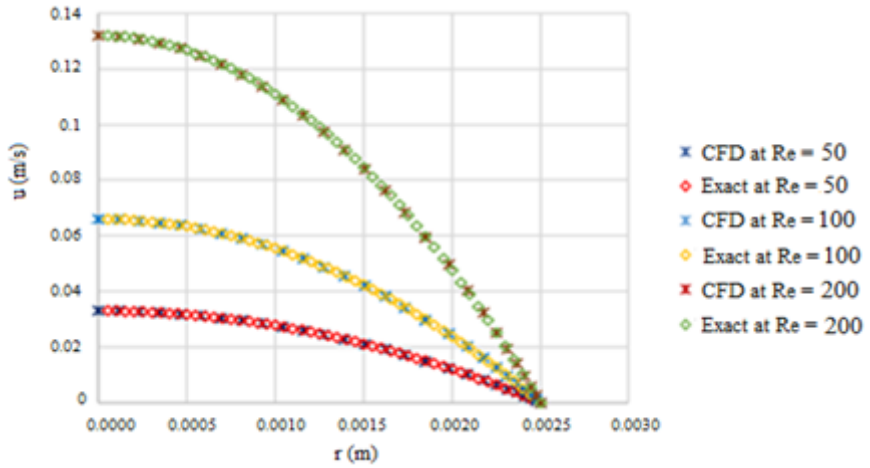

Fig. 4. velocity profile at different Reynolds number for Newtonian model in straight pipe (Density of blood 1060 kg/m^3 and viscosity 0.0035 Pa.s)

2.6.2 Validation of the non-Newtonian case

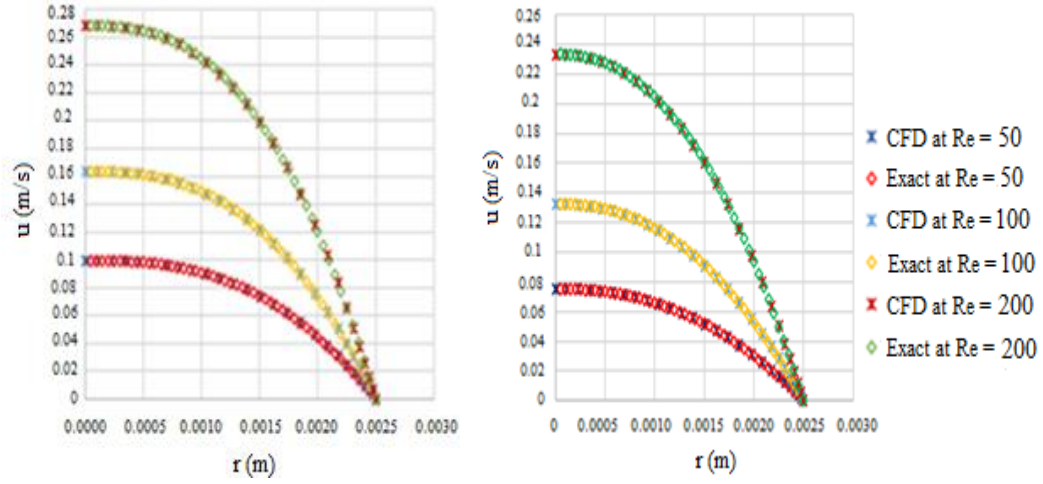

Fig. 5. velocity profile at different Reynolds number for the power-law model in straight pipe A) case 1 and B) case 2

3. Results and Discussion

A Newtonian model and two groups of Power-law model with different parameters have been simulated on the curved pipe at five different locations. Each of the three models simulated at three different Reynolds number ranged from (50 to 200) to clarify the effect of the rheological models (Newtonian and Power-law) on hemodynamic factors like the velocity profiles, the wall shear stress (WSS) and pressure drop per unit length.

3.1 Flow Structure and Velocity Profiles in Curved Pipe

Figures 6-10 show the velocity profiles of the curved pipe with different rheological models at different locations. Differences between the measured velocity distribution of the Newtonian and non-Newtonian fluid are evident. It can be noticed that the velocity profiles of the Newtonian model at Reynolds number ranging from 50 to 200 showed usual parabolic profiles. In addition, the two groups of the non-Newtonian model have similar behavior. However, there are quantitative differences recorded.

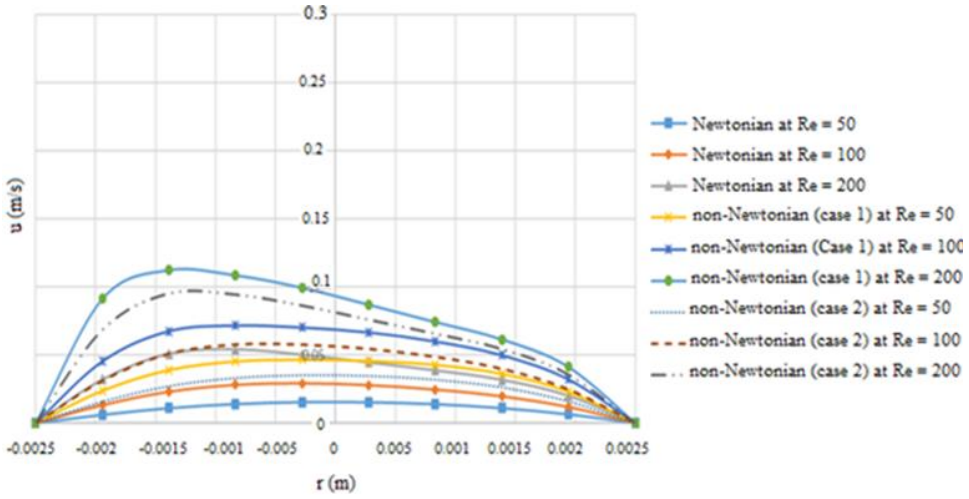

Fig. 6. Velocity profile at different Reynolds number for Newtonian and non-Newtonian models in curved pipe at location 1

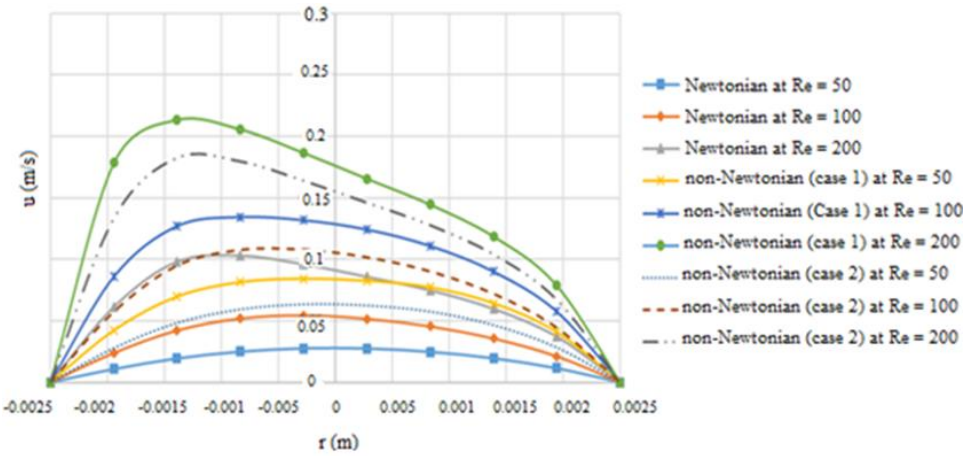

Fig. 7. Velocity profile at different Reynolds number for Newtonian and non-Newtonian models in curved pipe at location 2

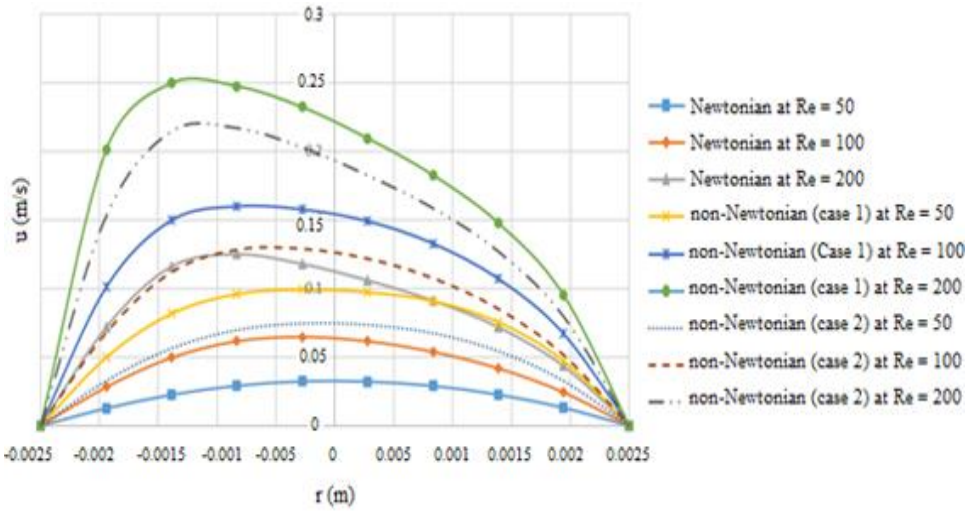

Fig. 8. Velocity profile at different Reynolds number for Newtonian and non-Newtonian models in curved pipe at location 3

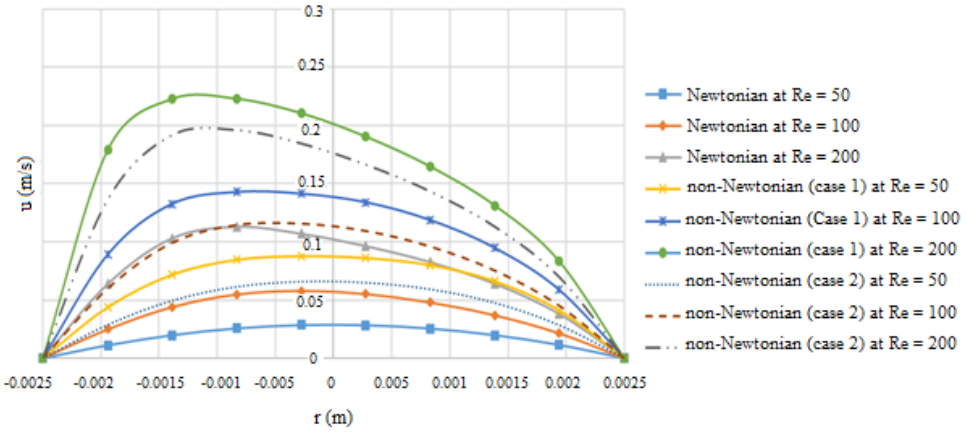

Fig. 9. Velocity profile at different Reynolds number for Newtonian and non-Newtonian models in curved pipe at location 4

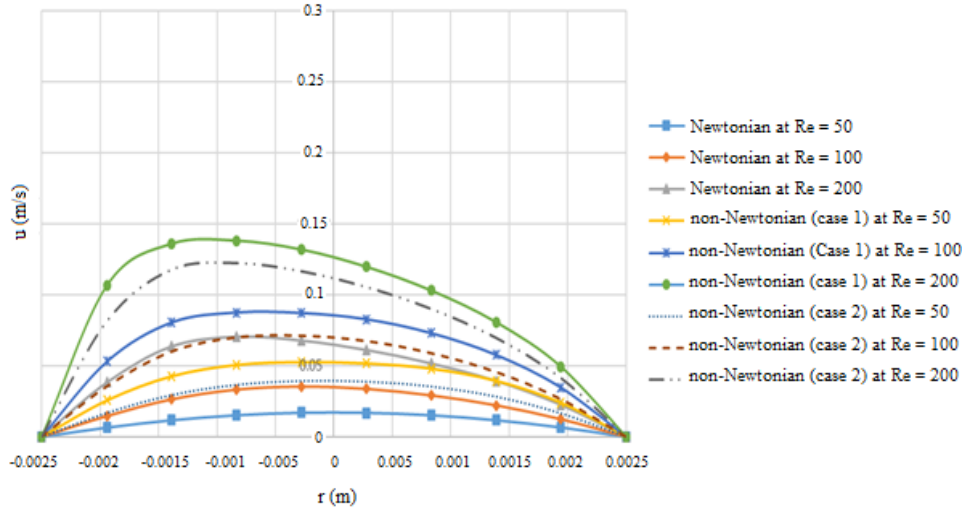

Fig. 10. Velocity profile at different Reynolds number for Newtonian and non-Newtonian models in curved pipe at location 5

The flow field for Re = 50 exhibits similar behaviour for all Newtonian and non-Newtonian solutions, which has axisymmetric profile in space. It is shown that the maximum velocity reached during the Newtonian solution is 0.033 m/s at location 3 ($90°$) while the minimum velocity reached is 0.015 m/s at the first location ($30°$). In addition, during the non-Newtonian solution such values increased. For case 1, the maximum velocity is 0.1 m/s at location 3 ($90°$), while the minimum velocity reached is 0.044 m/s at location 1 ($30°$). On the other hand, when increasing the power-law index in case 2 (n=0.7755), the velocity values decreased than case 1 (n=0.6) but still larger than the Newtonian solution. Starting from Re = 100, The flow field exhibits similar properties for Newtonian as such of Re = 50, however, this behaviour become axisymmetric pattern for both non-Newtonian cases. it is clear that the asymmetric behaviour of the instability region becomes more manifested at power-law index (n=0.6), as shown in Figures 6-10. The asymmetry in velocity profiles shown in Figures 6-10 was due to the influence of the Coriolis acceleration.

3.2 Wall Shear Stress Comparison between Newtonian and Non-Newtonian
3.2.1 Straight pipe

It is evident that the magnitude of the average WSS of the non-Newtonian model for both cases are greater than the Newtonian model in straight pipe as shown in Table 4. The deviation between them at Re =50 for case 1 is 84% while for case 2 is 75%. At Re=100, the deviation between the two rheological model is decreased for case 1 is 75% while at case 2 is 66%. At Re=200, the deviation between the Newtonian and the non-Newtonian model for case 1 is 67%, while for case 2, the deviation is 64%.

Table 4
The average wall shear stress of both Newtonian and non-Newtonian models in straight pipe

	Newtonian model	Non-Newtonian model (case 1)	Non-Newtonian model (case 2)	Deviation between Newtonian and non-Newtonian	Deviation between Newtonian and non-Newtonian
Re	WSS (Pa)	WSS (Pa)	WSS (Pa)	(case 1)	(case 2)
50	0.09238913	0.57531012	0.3908808	0.48292099	0.29849167
100	0.1847913	0.7743354	0.6063396	0.5895411	0.4215483
200	0.36961975	1.0422015	0.9405627	0.67258175	0.57094295

3.2.2 Curved pipe

Table 5 represents the average WSS of the Newtonian and both cases of the non-Newtonian models in the curved pipe. It is clear that the values are nearly similar to the straight pipe. The difference between the two geometries regarding the average WSS is 1%.

Table 5
The average wall shear stress of both Newtonian and non-Newtonian models in curved pipe

	Newtonian model	Non-Newtonian model (case 1)	Non-Newtonian model (case 2)	Deviation between Newtonian and non-Newtonian	Deviation between Newtonian and non-Newtonian
Re	WSS (Pa)	WSS (Pa)	WSS (Pa)	(case 1)	(case 2)
50	0.092516523	0.57935402	0.3924499	0.486837497	0.299933377
100	0.19052201	0.82062814	0.6347463	0.63010613	0.47295262
200	0.4256658	1.237555	1.1102546	0.8118892	0.6845888

It can be noted that the difference in WSS values between all cases is less prominent than for the velocity profiles. This difference is noticeable mostly in large Reynolds number.

3.3 Shear Rate Comparison between Newtonian and Non-Newtonian in Straight and Curved pipes

The shear rate of both non-Newtonian cases is greater than the Newtonian model as shown in Table 6. The high shear rate is present at the non-Newtonian model (case 1) which indicates that the flow is fast, while the Newtonian case is presented the low shear rate which means that the flow is slow at all values of Reynolds number and at a constant diameter for both geometry which is 5mm.

Table 6
The shear rate of both Newtonian and non-Newtonian models

	Shear rate Newtonian	Shear rate non-Newtonian (case 1)	Shear rate non-Newtonian (case 2)
Re	$\dot{\gamma}\ (1/s)$	$\dot{\gamma}\ (1/s)$	$\dot{\gamma}\ (1/s)$
50	26.4	79.76	60.24
100	52.8	131.2	106.4
200	105.6	214.4	186.4

3.4 Pressure Drop Comparison between Newtonian and Non-Newtonian

As a final comparison, the effect of shear-thinning model with respect to Newtonian model has been integrated by computing the pressure drop per unit length for both geometries at different Reynolds number as shown in Table 7 and 8. It is found that the pressure drop per unit length for the curved pipe is less than the straight pipe for both rheological models. However, it can be seen that the variation regarding the rheological models is greater than the variation regarding the geometry. It can be seen that the choice of blood rheology impacts the result of pressure drop. The pressure drop per unit length calculated from the non-Newtonian models was significantly greater than the obtained from the Newtonian case. This result reveals that the shear-thinning model have larger viscous forces than the Newtonian model and hence the blood rheology can play a perceptible role in the resulting computed pressure drop.

Table 7
The pressure drop per unit length of the Newtonian model and the non-Newtonian cases in straight pipe

	Newtonian model	Non-Newtonian model (case 1)	Non-Newtonian model (case 2)
Re	Δp (mPa/mm)	Δp (mPa/mm)	Δp (mPa/mm)
50	73.91963	460.30552	312.74418
100	147.86166	619.58694	485.17105
200	295.7867	833.98041	752.6723

Table 8
The pressure drop per unit length of the Newtonian model and the two cases of the non-Newtonian model in curved pipe

	Newtonian model	Non-Newtonian model (case 1)	Non-Newtonian model (case 2)
Re	Δp (mPa/mm)	Δp (mPa/mm)	Δp (mPa/mm)
50	70.61956	442.0148	299.4461
100	144.4571	619.922	479.9669
200	316.1621	919.2894	822.4815

It was found that the effect of the rheology with respect to the pressure drop per unit length is more significant than the impact of the geometry. For the Newtonian model, the maximum deviation

between the straight and curved pipe regarding the pressure drop per unit length at Re=200 was 6% while, for the non-Newtonian model (case 1) the maximum difference was 9% and that the difference between the straight and curved pipe for the non-Newtonian model (case 2) was 8%. Furthermore, it was shown that for the straight pipe the maximum deviation between the Newtonian and the power-law model (case 1) was 65% while between the Newtonian and power-law (case2) was 61%. For the curved pipe these values slightly increased by 1%. Thus, it was clearly shown that the non-Newtonian behaviour could not be neglected when simulating blood flow.

4. Conclusions

This study presents a numerical investigation of mean velocity profile for two simple geometries related to cerebral arteries using different rheological models, in order to compare between Newtonian and non-Newtonian models at low to medium shear rates. The comparative analysis shows that the geometry has a little impact on the rheological behaviour of blood at this range of shear rate. The major differences between the Newtonian and the non-Newtonian models are observed in the pressure drop per unit length. However, the deviation between the Newtonian and both cases of non-Newtonian model with respect to the WSS in both geometries was less prominent than the differences in the pressure drop per unit length. The found differences could not be neglected, therefore the non-Newtonian blood viscosity model should be taken into consideration for future blood flow studies in cerebral arteries. This work could be extended by simulating unsteady flow in curved pipe. Comparing unsteady flow simulations with the current study would provide a more complete insight into the influences of using the non-Newtonian model.

Acknowledgement

The authors would like to thank the Center for Information and Communication Technology (CICT) in Universiti Teknologi Malaysia for supporting and providing facilities and services of high-performance computing.

References

[1] Thurston, George B. "Rheological parameters for the viscosity viscoelasticity and thixotropy of blood." *Biorheology* 16, no. 3 (1979): 149-162. https://doi.org/10.3233/BIR-1979-16303

[2] Campo-Deaño, Laura, Mónica SN Oliveira, and Fernando T. Pinho. "A review of computational hemodynamics in middle cerebral aneurysms and rheological models for blood flow." *Applied Mechanics Reviews* 67, no. 3 (2015). https://doi.org/10.1115/1.4028946

[3] Carlier, Stéphane G., Luc CA van Damme, Casper P. Blommerde, Jolanda J. Wentzel, Glenn van Langehove, Stephan Verheye, Mark M. Kockx et al. "Augmentation of wall shear stress inhibits neointimal hyperplasia after stent implantation: inhibition through reduction of inflammation?." *Circulation* 107, no. 21 (2003): 2741-2746. https://doi.org/10.1161/01.CIR.0000066914.95878.6D

[4] Benard, Nicolas, Damien Coisne, Erwan Donal, and Robert Perrault. "Experimental study of laminar blood flow through an artery treated by a stent implantation: characterisation of intra-stent wall shear stress." *Journal of biomechanics* 36, no. 7 (2003): 991-998. https://doi.org/10.1016/S0021-9290(03)00068-X

[5] Cho, Young I., and Kenneth R. Kensey. "Effects of the non-Newtonian viscosity of blood on flows in a diseased arterial vessel. Part 1: Steady flows." *Biorheology* 28, no. 3-4 (1991): 241-262. https://doi.org/10.3233/BIR-1991-283-415

[6] Algabri, Yousif A., Surapong Chatpun, and Ishkrizat Taib. "An investigation of pulsatile blood flow in an angulated neck of abdominal aortic aneurysm using computational fluid dynamics." *Journal of Advanced Research in Fluid Mechanics and Thermal Sciences* 57, no. 2 (2019): 265-274.

[7] Jamali, Muhammad Sabaruddin Ahmad, and Zuhaila Ismail. "Simulation of Heat Transfer on Blood Flow through a Stenosed Bifurcated Artery." *Journal of Advanced Research in Fluid Mechanics and Thermal Sciences* 60, no. 2 (2019): 310-323.
[8] Pedley, Timothy J., and X. Y. Luo. *Fluid mechanics of large blood vessels*. Shaanxi People's Press, 1995.
[9] Kumar, K. Anantha, V. Sugunamma, and N. Sandeep. "Effect of thermal radiation on MHD Casson fluid flow over an exponentially stretching curved sheet." *Journal of Thermal Analysis and Calorimetry* (2019): 1-9.
[10] Anantha Kumar, Kempannagari, Vangala Sugunamma, and Naramgari Sandeep. "Physical aspects on unsteady MHD-free convective stagnation point flow of micropolar fluid over a stretching surface." *Heat Transfer—Asian Research* 48, no. 8 (2019): 3968-3985. https://doi.org/10.1002/htj.21577
[11] Kumar, K. Anantha, V. Sugunamma, and N. Sandeep. "A non-Fourier heat flux model for magnetohydrodynamic micropolar liquid flow across a coagulated sheet." *Heat Transfer—Asian Research* 48, no. 7 (2019): 2819-2843. https://doi.org/10.1002/htj.21518
[12] Kumar, K. Anantha, V. Sugunamma, N. Sandeep, and M. T. Mustafa. "Simultaneous solutions for first order and second order slips on micropolar fluid flow across a convective surface in the presence of Lorentz force and variable heat source/sink." *Scientific reports* 9, no. 1 (2019): 1-14. https://doi.org/10.1038/s41598-019-51242-5
[13] Mahrous, Samar A., Nor Azwadi Che Sidik, and Khalid M. Saqr. "Newtonian and non-Newtonian CFD Models of Intracranial Aneurysm: A Review." *CFD Letters* 12, no. 1 (2020): 62-86.
[14] Ferroudji, Hicham, Ahmed Hadjadj, Mohammad Azizur Rahman, Ibrahim Hassan, Titus Ntow, and Ahmed Haddad Ofei. "The Impact of Orbital Motion of Drill Pipe on Pressure Drop of Non-Newtonian Fluids in Eccentric Annulus."
[15] Rojas, Hernán A. González. "Numerical implementation of viscoelastic blood flow in a simplified arterial geometry." *Medical engineering & physics* 29, no. 4 (2007): 491-496. https://doi.org/10.1016/j.medengphy.2006.07.002
[16] Lerche, Dietmar, Georgios Vlastos, Brigitte Koch, Manfred Pohl, and Klaus Affeld. "Viscoelastic behaviour of human blood and polyacrylamide model fluids for heart valve testing." *Journal de Physique III* 3, no. 6 (1993): 1283-1289. https://doi.org/10.1051/jp3:1993198
[17] Burleson, Arrmelle C., and Vincent T. Turitto. "Identification of quantifiable hemodynamic factors in the assessment of cerebral aneurysm behavior on behalf of the subcommittee on biorheology of the scientific and standardization committee of the ISTH." *Thrombosis and haemostasis* 75, no. 01 (1996): 118-123. https://doi.org/10.1055/s-0038-1650533
[18] Singh, Pankaj K., Alberto Marzo, Bethany Howard, Daniel A. Rufenacht, Philippe Bijlenga, Alejandro F. Frangi, Patricia V. Lawford, Stuart C. Coley, D. Rodney Hose, and Umang J. Patel. "Effects of smoking and hypertension on wall shear stress and oscillatory shear index at the site of intracranial aneurysm formation." *Clinical neurology and neurosurgery* 112, no. 4 (2010): 306-313. https://doi.org/10.1016/j.clineuro.2009.12.018
[19] Shojima, Masaaki, Shigeru Nemoto, Akio Morita, Marie Oshima, Eiju Watanabe, and Nobuhito Saito. "Role of shear stress in the blister formation of cerebral aneurysms." *Neurosurgery* 67, no. 5 (2010): 1268-1275. https://doi.org/10.1227/NEU.0b013e3181f2f442
[20] Evju, Øyvind, Kristian Valen-Sendstad, and Kent-André Mardal. "A study of wall shear stress in 12 aneurysms with respect to different viscosity models and flow conditions." *Journal of biomechanics* 46, no. 16 (2013): 2802-2808. https://doi.org/10.1016/j.jbiomech.2013.09.004
[21] Xiang, Jianping, Markus Tremmel, John Kolega, Elad I. Levy, Sabareesh K. Natarajan, and Hui Meng. "Newtonian viscosity model could overestimate wall shear stress in intracranial aneurysm domes and underestimate rupture risk." *Journal of neurointerventional surgery* 4, no. 5 (2012): 351-357. https://doi.org/10.1136/neurintsurg-2011-010089
[22] Morales, Hernán G., Ignacio Larrabide, Arjan J. Geers, Martha L. Aguilar, and Alejandro F. Frangi. "Newtonian and non-Newtonian blood flow in coiled cerebral aneurysms." *Journal of biomechanics* 46, no. 13 (2013): 2158-2164. https://doi.org/10.1016/j.jbiomech.2013.06.034
[23] Cavazzuti, Marco, Mark Atherton, Michael Collins, and Giovanni Barozzi. "Beyond the virtual intracranial stenting challenge 2007: non-Newtonian and flow pulsatility effects." *Journal of biomechanics* 43, no. 13 (2010): 2645-2647. https://doi.org/10.1016/j.jbiomech.2010.04.042
[24] Cavazzuti, Marco, M. A. Atherton, M. W. Collins, and Giovanni Sebastiano Barozzi. "Non-Newtonian and flow pulsatility effects in simulation models of a stented intracranial aneurysm." *Proceedings of the Institution of Mechanical Engineers, Part H: Journal of Engineering in Medicine* 225, no. 6 (2011): 597-609. https://doi.org/10.1177/09544119JEIM894

[25] Fisher, Carolyn, and Jenn Stroud Rossmann. "Effect of non-Newtonian behavior on hemodynamics of cerebral aneurysms." *Journal of biomechanical engineering* 131, no. 9 (2009). https://doi.org/10.1115/1.3148470
[26] Johnston, Barbara M., Peter R. Johnston, Stuart Corney, and David Kilpatrick. "Non-Newtonian blood flow in human right coronary arteries: transient simulations." *Journal of biomechanics* 39, no. 6 (2006): 1116-1128. https://doi.org/10.1016/j.jbiomech.2005.01.034
[27] Rodkiewicz, C. M., Prawal Sinha, and J. S. Kennedy. "On the application of a constitutive equation for whole human blood." *Journal of biomechanical engineering* 112, no. 2 (1990): 198-206. https://doi.org/10.1115/1.2891172
[28] Tu, Cheng, and Michel Deville. "Pulsatile flow of non-Newtonian fluids through arterial stenoses." *Journal of biomechanics* 29, no. 7 (1996): 899-908. https://doi.org/10.1016/0021-9290(95)00151-4
[29] Gijsen, F. J. H., E. Allanic, F. N. Van de Vosse, and J. D. Janssen. "The influence of the non-Newtonian properties of blood on the flow in large arteries: unsteady flow in a 90 curved tube." *Journal of biomechanics* 32, no. 7 (1999): 705-713. https://doi.org/10.1016/S0021-9290(99)00014-7
[30] Perktold, Karl, R. Peter, and Michael Resch. "Pulsatile non-Newtonian blood flow simulation through a bifurcation with an aneurysm." *Biorheology* 26, no. 6 (1989): 1011-1030. https://doi.org/10.3233/BIR-1989-26605
[31] Ballyk, P. D., D. A. Steinman, and C. R. Ethier. "Simulation of non-Newtonian blood flow in an end-to-side anastomosis." *Biorheology* 31, no. 5 (1994): 565-586. https://doi.org/10.3233/BIR-1994-31505
[32] Marossy, A., P. Švorc, I. Kron, and S. Grešová. "Hemorheology and circulation." *Clinical hemorheology and microcirculation* 42, no. 4 (2009): 239-258. https://doi.org/10.3233/CH-2009-1192
[33] Pohl, Manfred, Max Otto Wendt, Sabine Werner, Brigitte Koch, and Dietmar Lerche. "In vitro testing of artificial heart valves: comparison between Newtonian and non-Newtonian fluids." *Artificial organs* 20, no. 1 (1996): 37-46. https://doi.org/10.1111/j.1525-1594.1996.tb04416.x
[34] Liu, Xiao, Yubo Fan, Xiaoyan Deng, and Fan Zhan. "Effect of non-Newtonian and pulsatile blood flow on mass transport in the human aorta." *Journal of biomechanics* 44, no. 6 (2011): 1123-1131. https://doi.org/10.1016/j.jbiomech.2011.01.024
[35] Kumar, D., R. Vinoth, and Vijay Shankar Raviraj Adhikari. "Non-Newtonian and Newtonian blood flow in human aorta: a transient analysis." *An Internayional Journal of Medical Sciences* 28, no.7 (2017).
[36] Kwon, Ohwon, Mahesh Krishnamoorthy, Young I. Cho, John M. Sankovic, and Rupak K. Banerjee. "Effect of blood viscosity on oxygen transport in residual stenosed artery following angioplasty." *Journal of Biomechanical Engineering* 130, no. 1 (2008). https://doi.org/10.1115/1.2838029
[37] Mejia, Juan, Rosaire Mongrain, and Olivier F. Bertrand. "Accurate prediction of wall shear stress in a stented artery: Newtonian versus non-Newtonian models." *Journal of biomechanical engineering* 133, no. 7 (2011). https://doi.org/10.1115/1.4004408
[38] Jeong, W. W., and K. Rhee. "Effects of surface geometry and non-newtonian viscosity on the flow field in arterial stenoses." *Journal of mechanical science and technology* 23, no. 9 (2009): 2424-2433. https://doi.org/10.1007/s12206-009-0627-6
[39] Kulcsár, Zsolt Mihály. "Role of hemodynamics in the life cycle of cerebral aneurysm." 2011.
[40] Cebral, Juan R., Marcelo A. Castro, James E. Burgess, Richard S. Pergolizzi, Michael J. Sheridan, and Christopher M. Putman. "Characterization of cerebral aneurysms for assessing risk of rupture by using patient-specific computational hemodynamics models." *American Journal of Neuroradiology* 26, no. 10 (2005): 2550-2559.
[41] Lindekleiv, Haakon M., Kristian Valen-Sendstad, Michael K. Morgan, Kent-Andre Mardal, Kenneth Faulder, Jeanette H. Magnus, Bertil Romner, and Tor Ingebrigtsen. "Sex differences in intracranial arterial bifurcations." *Gender medicine* 7, no. 2 (2010): 149-155. https://doi.org/10.1016/j.genm.2010.03.003
[42] Campo-Deaño, Laura, Mónica SN Oliveira, and Fernando T. Pinho. "A review of computational hemodynamics in middle cerebral aneurysms and rheological models for blood flow." *Applied Mechanics Reviews* 67, no. 3 (2015). https://doi.org/10.1115/1.4028946
[43] Molla, M. Mamun, and M. C. Paul. "LES of non-Newtonian physiological blood flow in a model of arterial stenosis." *Medical engineering & physics* 34, no. 8 (2012): 1079-1087. https://doi.org/10.1016/j.medengphy.2011.11.013

[44] Husain, Iqbal, Fotini Labropulu, Chris Langdon, and Justin Schwark. "A comparison of Newtonian and non-Newtonian models for pulsatile blood flow simulations." *Journal of the Mechanical Behaviour of Materials* 21, no. 5-6 (2013): 147-153.

[45] Frolov, S. V., S. V. Sindeev, D. Liepsch, and A. Balasso. "Experimental and CFD flow studies in an intracranial aneurysm model with Newtonian and non-Newtonian fluids." *Technology and Health Care* 24, no. 3 (2016): 317-333.
https://doi.org/10.3233/THC-161132

[46] Frolov, S. V., S. V. Sindeev, D. Liepsch, A. Balasso, P. Arnold, J. S. Kirschke, S. Prothmann, and A. Yu Potlov. "NEWTONIAN AND NON-NEWTONIAN BLOOD FLOW AT A 90∘-BIFURCATION OF THE CEREBRAL ARTERY: A COMPARATIVE STUDY OF FLUID VISCOSITY MODELS." *Journal of Mechanics in Medicine and Biology* 18, no. 05 (2018): 1850043.
https://doi.org/10.1142/S0219519418500434

[47] Yamaguchi, H. "Mechanics of Engineering Fluids." (2008).

[48] Madlener, K., B. Frey, and H. K. Ciezki. "Generalized reynolds number for non-newtonian fluids." *Progress in Propulsion Physics* 1 (2009): 237-250.
https://doi.org/10.1051/eucass/200901237

[49] Jamous, Mohammad A., Shinji Nagahiro, Keiko T. Kitazato, Tetsuya Tamura, Hani Abdel Aziz, Masayuki Shono, and Koichi Satoh. "Endothelial injury and inflammatory response induced by hemodynamic changes preceding intracranial aneurysm formation: experimental study in rats." *Journal of neurosurgery* 107, no. 2 (2007): 405-411.
https://doi.org/10.3171/JNS-07/08/0405

[50] Moore, James E., Chengpei Xu, Seymour Glagov, Christopher K. Zarins, and David N. Ku. "Fluid wall shear stress measurements in a model of the human abdominal aorta: oscillatory behavior and relationship to atherosclerosis." *Atherosclerosis* 110, no. 2 (1994): 225-240.
https://doi.org/10.1016/0021-9150(94)90207-0

[51] Schirmer, Clemens M., and Adel M. Malek. "Critical influence of framing coil orientation on intra-aneurysmal and neck region hemodynamics in a sidewall aneurysm model." *Neurosurgery* 67, no. 6 (2010): 1692-1702.
https://doi.org/10.1227/NEU.0b013e3181f9a93b